RESEARCH ARTICLE   OPEN ACCESS

Aerodynamic Drag Reduction for A Generic Sport Utility Vehicle Using Rear Suction

Abdellah Ait Moussa*, Rohan Yadav* and Justin Fischer*

*(Department of Engineering and Physics, University of Central Oklahoma, 100 North University Drive, Edmond, Oklahoma, USA 73034. Email: aaitmoussa@uco.edu)

ABSTRACT
The high demand for new and improved aerodynamic drag reduction devices has led to the invention of flow control mechanisms and continuous suction is a promising strategy that does not have major impact on vehicle geometry. The implementation of this technique on sport utility vehicles (SUV) requires adequate choice of the size and location of the opening as well as the magnitude of the boundary suction velocity. In this paper we introduce a new methodology to identifying these parameters for maximum reduction in aerodynamic drag. The technique combines automatic modeling of the suction slit, computational fluid dynamics (CFD) and a global search method using orthogonal arrays. It is shown that a properly designed suction mechanism can reduce drag by up to 9%..

*Keywords-*Aerodynamics, Fluid dynamics, Optimization, Taguchi Method, CFD based optimization

I. INTRODUCTION

The rapidly increasing fuel prices as well as the new and enforced regulations to control the discharge of greenhouse gases have raised lots of constraints on the automobile makers. SUVs in particular are known for their larger drag coefficients because of their boxy shaped geometry and the extent to which factors such as flow separation and reattachment, vortex shedding, skin friction and separated vortices in the near wake region have on the overall aerodynamic performance [1-6]. Careful and well-engineered vehicle design isimperative and new and improved design tools are essential.

In a previous study [7], it was shown that Significant improvement in aerodynamic drag can be achieved if small chamfers are made at the rear end of the roof and the side body of an SUV, and when the foot step of the vehicle is moved downward to decrease ground clearance near the wheels. Furthermore, lowering the front bumper and bonnet, tilting the front windshield, rounding off the corners and sharp edges, and lastly extending the front bumper are all ways to improving vehicle aerodynamics. In spite of all these tips, aerodynamic drag is essentially still a relevant factor for most SUVs and there is still room for improvement.

The use of add-on devices was another resort that the automobile industry turned to. In a study over the Ahmed reference model [8], a boat tail flap in the rear end of the vehicle was proven to appreciably improve aerodynamic performance. Few of these additional devices are already in use in a number of cars and SUV models. In the same sense, the use of external energy sources to modify the near wall flow without necessarily modifying the shape of the vehicle is

another promising strategy [9]. Flow control was extensively studied and applied [10-12]. Different mechanisms were analyzed and tested in academic and industrial laboratories and the results were all encouraging. Continuous suction [13-14] offers a promising alternative and seems well adapted to the automobile context.

Engineering problems are usually multi-variable, multi-constraint problems, and attempting to adopt full factorial experiments or simulations is definitely not cost effective. Furthermore, the analysis must take into account the details of the geometry rather than a simplified model, since small changes in any of the geometrical parameters of the vehicle may lead to larger changes in the aerodynamic flow around it. Rather than manually iterating design changes whether experimentally or via simulation until all design requirements are met, an engineer can work more effectively by automating the design and simulation processes and allow an optimization algorithm to create a final design that meets the particular requirements. The technique introduced in this paper is based on this perception and will be discussed in more details in the next few sections.

This paper is divided into three major parts. In the first, we introduce the technique of optimization and components used in the process of computing and minimizing drag. Next, we discuss the results of the suction mechanism on the overall aerodynamic performance of the vehicle. In the final section we conclude with a summary and a discussion of future work.

II. THECOMPUTATIONAL TECHNIQUE

In this section, we shall describe the general structure of the computational technique that we apply to a specific SUV model.

II.1 The Physical Model

A pictorial representational of the SUV model used in the present analysis is shown in Fig.1. The physical model is 1/10th scale generic SUV without side mirrors. The overall length, width and height were $L_v = 432$ mm, $W_v = 152$ mm and $H_v = 148$ mm, respectively. Arectangular slit was added and merged at the rear of the vehicle. The slit length (L_s), width (W_s)and centroid vertical coordinate (Y_c) were all normalized with reference to the vehicle height (H_v). Air is sucked uniformly through the slit and the boundary inlet velocity (V_s) together with (L_s, W_s, Y_c) were considered as the design variables.

In the next section, we introduce the technique used to identify the optimal values of the design variables for maximum reduction in aerodynamic drag.
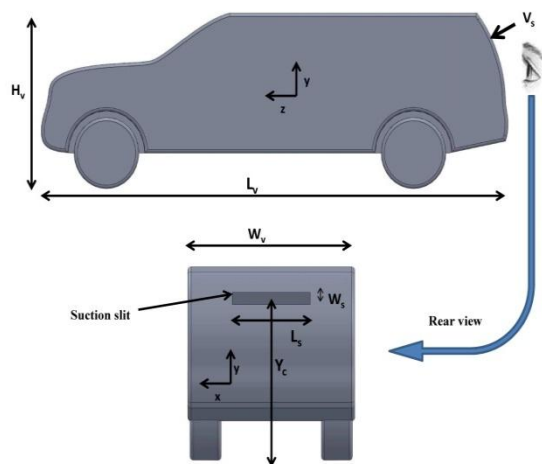

Figure 1: Physical model

II.2 The optimization Technique

Orthogonal array optimization or Taguchi method [15-17] isa statistical technique used to study the simultaneouseffect of multiple variables on the performance of a process.It was developed by Genichi Taguchi from Japanduring late 1940. When first proposed, Taguchi showedthat design of experiments (DOE) could be used to improve thequality of manufactured products. He suggested that fractionalfactorial experiments provide a mean to cost effectively investigate complex problems. Taguchi devised a numberof special orthogonal arrays, each of which is used for anumber of experimental situations. In these tables thevariables or factors are arranged such that between anypair of columns each combination of levels appears an equal number of times. He proposed a way ofanalyzing the

experimental results and identifying the bestquality process to be used. Design of experiments using the Taguchi approach is very effective for product developmentand industrial engineering and has been successfullyapplied in numerous research areas [18 - 20]. In the current development, we use Taguchi's technique and orthogonal arrays to identify the set of design parameters, (L_s, W_s, Y_c, V_s), that maximize the reduction in aerodynamic drag.

The Taguchi technique requires, in addition to the design variables (factors), a list of levels for each factor. The number of factors and their levels determine the orthogonal array to be used. In the current analysis three levels were identified for each of the four factors and an L9 orthogonal array is used to identify the best design parameters.

Strictly speaking, in an engineering problem such as the one we are currently facing, the design variables $(x_1, x_2, x_3, ...)$ may vary over a constrained continuum (i.e.box constraints: $x_i^{lower\ bound} < x_i < x_i^{upper\ bound}$), and opting to identify the factor levels by only three set of values may not lead to the best optimal solution. A global search however, can be performed by repeatedly restarting the Taguchi algorithm over the domain of analysis. To avoid finding the same local optima, the factor levels should be different and preferably far from previous known local solutions. To this end, we use a variable variance probability density (VVP) [21] to identify levels reasonably far from the known local minima then restart the Taguchi algorithm for the next optimum. More detail about the VVP can be found in the appendix.

The diagram in Fig.2 represents the scheme used in the implementation of the Taguchi method and the repetitive restarts needed to reach global optimum. We start with a fixed number of random vertices over the box constraint; each vertex encompasses one single level of each factor. We then identify the vertex with the largest probability density. The next two levels of each factor in the vertex (x_i^2, x_i^3) are calculated according to Eq.1, where (Δx_i)refers to the size of the domain of analysis of variable (x_i). We then proceed with the Taguchi algorithm and identify the most optimal vertex for drag reduction. There may be cases however, when the new optimum is identical to one of the stored optima; that the suggested optimum is not better than the best current vertex; or that one or more of the vertex levels are not on the box constraint. In cases like these we proceed as indicated in the diagram

$$x_i^k = x_i + 0.1 * (-1)^k \Delta x_i \ , \ k = 1, 2 \qquad (1)$$

The box projection procedure in Eq.2 assures that the levels are always selected over the domain of the analysis.

$$x_i = \begin{cases} x_i^{\text{lower bound}} & \text{if } x_i < x_i^{\text{lower bound}} \\ x_i^{\text{upper bound}} & \text{if } x_i > x_i^{\text{upper bound}} \end{cases} \quad (2)$$

where x_i is a level sampled during the optimization.

II.3 Program Structure

To achieve optimal values of drag coefficient [1], we will be facing three parts of work; geometric modelling, finiteelement analysis (FEA) and mathematical programming. Different program files were developed for each part, and communication between these parts is manipulated by an interface. One of the advantages of using the ANSYS Workbench software is the possibility to use it as a mere subroutine of any other external program, parameters can be either directly passed or exchanged through external files. This flexibility allows us to build an interface between ANSYS and our external optimization algorithm, written in Visual Basics for application (VBA), where ANSYS is a finite element package used to calculate the drag coefficient. For geometrical updates of all of (L_s, W_s, Y_c), we automated the SolidWorks Application Programming Interface (API) calls directly from our external optimization algorithm.The methodology schematics are shown in Fig.3. In the following the main parts are outlined.

Commands for updating the geometrical variables (L_s, W_s, Y_c), for generating and storing the parasolid model are incorporated in a SolidWorks macro. This list of API calls is directly implemented into the optimization algorithm written in VBA.

Commands for uploading the parasolid model, for adding an enclosure to simulate fluid flow and for applying a Boolean operation to subtract the geometry of the truck from the enclosure are incorporated in a command file using the Java Python language for the ANSYS Design Modeler.

Commands for meshing, for adding inflation on the road and truck surfaces and for applying body sizing and named selection are incorporated in a command file using the Java Python language for the ANSYS Mesher.

Commands for initializing the Fluent computation and applying boundary conditions including the boundary suction inlet velocity (V_s) are incorporated in a Fluent journal file. The script is automatically updated as new suction velocities are selected. Upon completion of the pre and post-processing stages, ANSYS provides results file which records the drag coefficient over the steps of the simulation, this information is stored in a files.out and returned to the interface. Communication with the ANSYS Workbench is made possible via a Workbench journal file.

For parametric optimization, we used the Taguchi method and orthogonal arrays in addition to the box constrained variable. The input parameters are read from an excel sheet. Results and geometrical updates are printed out on the same sheet to show optimization progress.

II.4 Finite Element Analysis Setup and Procedure

We used the Fluent analysis system in ANSYS Workbench. The model including the suction slit were imported to the Design modeler, and aligned with a control volume. A half model was used to allow quicker solution of the model with a more refined mesh. The control volume size was set according to Fluent's best practice guide for vehicle analysis [22]. The computational domain in Fig.4 extended around three times the vehicle length to the front and five times to the rear. The width and height of the control volume were set so that the cross section of the vehicle did not exceed 1.5% of the domain area. A box was created around the vehicle and in the wake region to control the mesh size during the meshing process. The box extended about half a vehicle length in front, to the sides and to the top, and about a vehicle length in the wake. The model was then subtracted from the computational domain to limit the computational analysis to the rest of the control volume and vehicle boundaries.
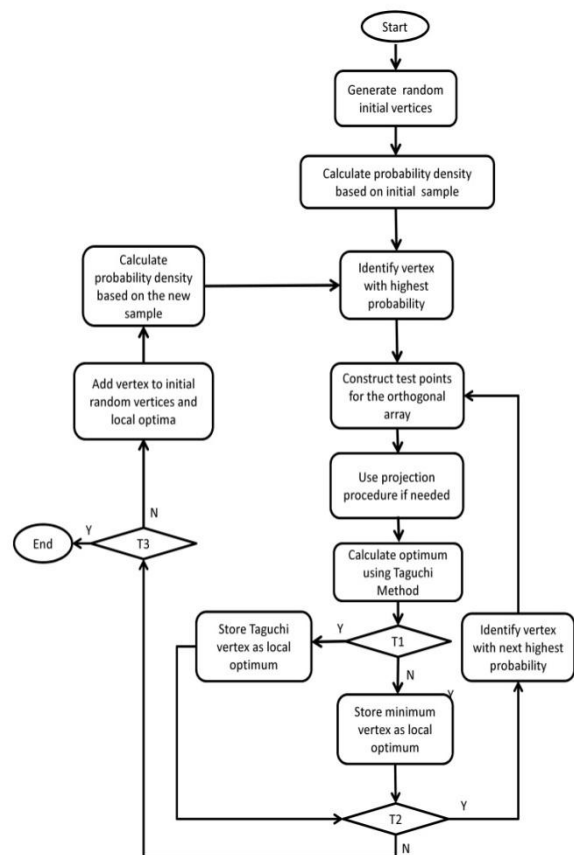

Figure 2: Global optimization. T1: (Taguchi suggested optimum is best), T2: (Already know as an optimum), T3: (maximum number of analyses is reached).
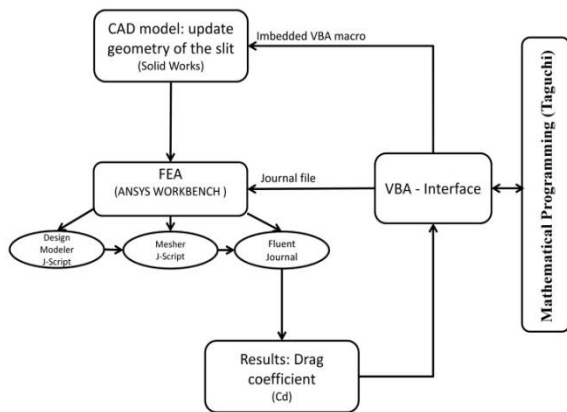
Figure 3: Program structure

TABLE I: GRID INDEPENDENCE TEST

Total number of cells	Drag coefficient	Convergence time
Medium (1909481 million)	0.4602	75 minutes
Fine$_1$ (3204109 million)	0.4676	120 minutes
Fine$_2$ (6432167 million)	0.4692	210 minutes

Figure 4: Simulation Box

Based on the analysis system utilized, the Mesher in ANSYS Workbench uploads a set of default parameters that will result in a mesh that is more favorable to the solver used. By means of global and local mesh controls, the user can easily modify the mesh parameters. In this paper we adopted a physicsbased meshing, the physics preference was set to CFD and solver to Fluent. An inflation layer was added over the surfaces of the vehicle and the road as shown in Fig.5; the prisms were grown with a first aspect ratio of 10 and a growth factor of 1.2 extruding 5 layers. Body sizing was used for mesh refinement around the vehicle and wake region. Triangular mesh elements were used on the surface to reduce the numerical diffusion and to align with the real flow near the model. The remainder of the computational domain was filledwith tetrahedral volume cells that were adjacent to the prism layers.

A velocity-inlet boundary condition was used to model the incoming flow as well as the suction inlet flow.Fluent's best practice guide for vehicle analysis [22] recommends using a Realizable k-epsilon Model, and non-equilibriumwall-functions(NWFs).Fluent convergence criterion of 10^{-4} for the continuity and momentum equations was used.

A grid independence test was performed on the unmodified geometry and the drag coefficient and convergence time were selected as the criteria. Six nodes were used in parallel computation to conduct the FEA simulation. Referring to the results in Table.I, as the mesh became finer; the drag coefficient reached an asymptotic value. Balance between calculation, time and the accuracy order of the simulation has been made and the setting for the "Fine$_1$" grid is considered to be sufficiently reliable.
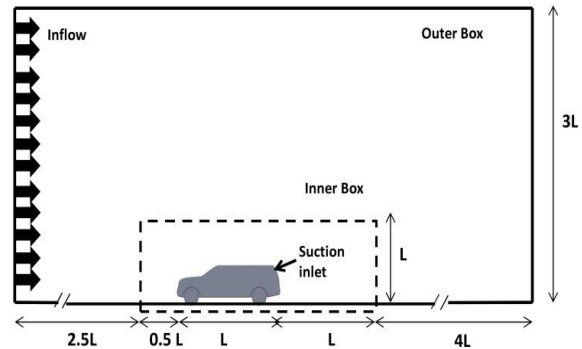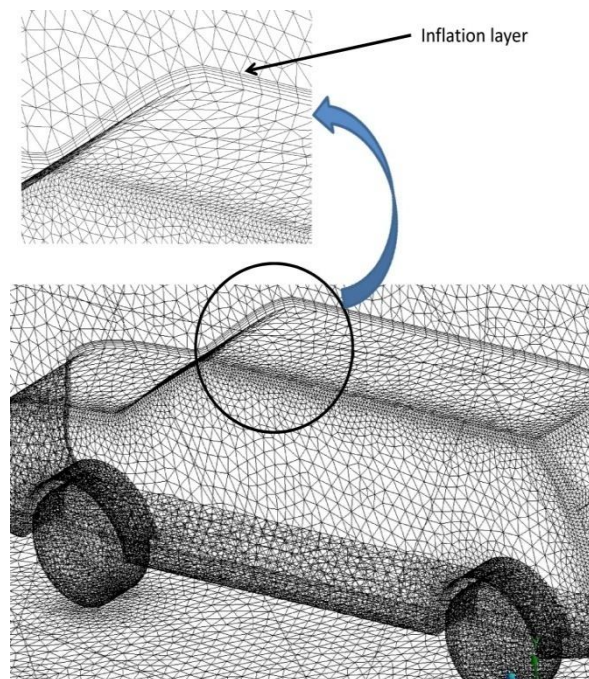

Figure 5: Boundary layer at a growth factor of 1.2, triangular mesh elements on the surface and tetrahedral volume cells in the reminder of the computational domain

III. RESULTS AND DISCUSSION
III.1Optimization Setup

The methodology was performed on the SUV model depicted in Fig.1. The maximum number of iterations in the global optimization procedure was set to 30. The box constraints for the design parameters were set according to Eq.3. The free stream velocity

was set to (V_∞ = 30 m/s), and the Reynolds number calculated based on the overall model length was Re = 7.95×10^5. We started with 10 random initial vertices over the box constraints, and the optimum points were rounded off to 10^{-2}.

$$\begin{cases} 0.07 \leq \dfrac{W_s}{H_v} \leq 0.2 \\ 0.26 \leq \dfrac{L_s}{H_v} \leq 0.92 \\ 0.39 \leq \dfrac{Y_c}{H_v} \leq 0.72 \\ 0 \leq \dfrac{V_s}{V_\infty} \leq 0.27 \end{cases} \quad (3)$$

III.2 Results and Discussion

Although we have over 25 configurations that the designer can choose from, the majority did not contribute equally toward the reduction of aerodynamic drag. For brevity, we displayed 7 of the calculated vertices since they seem to convey the general development of the analysis. Table.II, shows that reduction in aerodynamic drag can be achieved at different values of the design parameters which is an important feature especially for multi-objective optimization. To assess the relative influence of the different factors to the variation of the result we performed an analysis of variance (ANOVA) [15] over the vertices that led to the first result (row 1) in Table.II. Table III summarizes the results of the ANOVA analysis. These results were extracted from the ANOVA Table in Qualitek-4 [15]. We find that the factor influence of the % drag reduction decreases in the order ($V_s > Y_c > L_s > W_s$). Accordingly, the suction inlet velocity has more influence than the rest of the design variables.

TABLE II: OPTIMUM DESIGN OBTAINED BY ORTHOGONAL ARRAYS

$\dfrac{W_s}{H_v}$	$\dfrac{L_s}{H_v}$	$\dfrac{Y_c}{H_v}$	$\dfrac{V_s}{V_\infty}$	% reduction
0.20	0.92	0.53	0.05	8.1
0.16	0.53	0.72	0.03	7.9
0.11	0.79	0.68	0.03	7.2
0.11	0.79	0.68	0.17	6.2
0.09	0.79	0.54	0.10	5.8
0.20	0.39	0.61	0.21	5.4
0.14	0.53	0.51	0.16	4.1

TABLE III: ANOVA TABLE: FACTORS AND PERCENT OF INFLUENCE

Factors	% of influence
$\dfrac{W_s}{H_v}$	7.079
$\dfrac{L_s}{H_v}$	10.931
$\dfrac{Y_c}{H_v}$	14.527
$\dfrac{V_s}{V_\infty}$	38.899

To understand how the continuous suction affected the flow around the vehicle we displayed the velocity streamlines over the symmetry plane in Fig.6 (without suction) and Fig.7 (with suction). It can be seen that the lower recirculating flow behind the SUV was reduced and its core shifted slightly away toward the wake due to the inclusion of suction. The lesser the recirculation, the better the pressure build up below the suction inlet. This result is also confirmed in Fig.8 where the pressure coefficient (C_p) is plotted as a function of the normalized height. The pressure gain in the lower part of the suction slit outweighed the loss in pressure above the opening. Overall, the inclusion of suction reduced the pressure difference between the fore and after facing surfaces of the vehicle which thereby reduced drag.
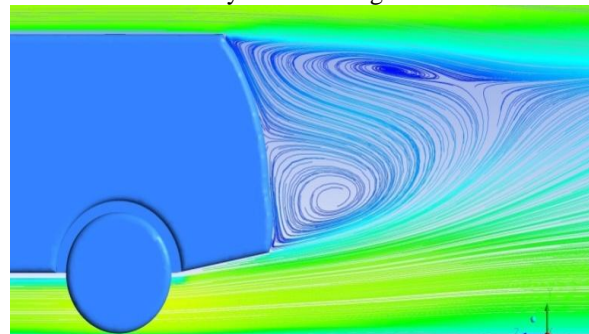

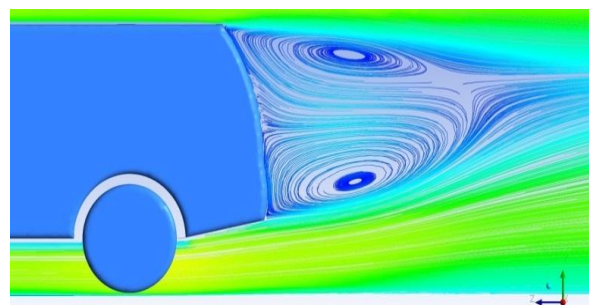Figure 6: Streamlines colored by the pressure coefficient (no suction)

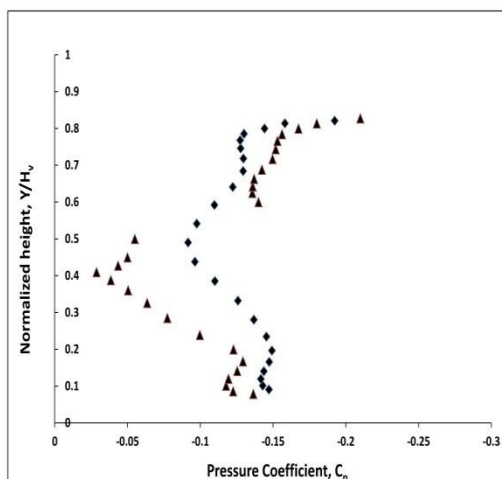Figure 7: Streamlines colored by the pressure coefficient (with suction)

Figure 8: Pressure coefficient distribution (Cp) on the symmetry plane over the back surface of the SUV, the height (Y) is measured from the truck

IV. Conclusion

In this paper, we investigated the effect of adding a suction slit in the rear of a generic model of an SUV on its overall aerodynamic performance. We introduced a robust method to identifying the size, location and boundary suction inlet velocity for maximum reduction in aerodynamic drag. The evolutionary aspect of the method delivered a family of solution that the designer can choose from. Proper design of the opening must take into account the actual geometry of the vehicle rather than simple models since small changes in geometrical details can lead to large changes in the aerodynamic flow around the vehicle. The methodology introduced in this paper made this quest achievable and cost effective.

The core of the analysis is the finite element simulation which is based on models that were proven to reproduce the general flow pattern but may miss some details that were only possible to identify by experimentation. Final tuning and adjustment are ultimately needed to finalize and benchmark our simulation results.

V. Acknowledgments

Appendix: *Variable Variance Probability Density (VVP)*

The variable variance probability (VVP) density is based on the minimum distance to the points already sampled and is represented as

$$\Phi(x) = \frac{1}{\sqrt{2\pi}\sigma}\left(1 - e^{d_{min}^2/2\sigma^2}\right) \qquad (A1)$$

$$d_{min} = \underset{i=1,\ldots,m}{min}\left\{d_i = \sqrt{\sum_{k=1}^{n}\left(\frac{x_{k,i} - x_k}{x_{k,u} - x_{k,l}}\right)^2}\right\}$$

Where $\Phi(x)$ is the sampling probability of a point x, n is the number of design variables, xi is a point previously sampled, and m is the number of points already sampled. Length di is the non-dimensional distance between point x and point xi.

The variance of the normal probability density, which is updated in each restart, is given by:

$$\sigma = \frac{1}{3\sqrt[n]{m}} \qquad (A2)$$

The variance is gradually decreasing when the number of sampled points is increased.

References

[1] Hucho, W.H., *Aerodynamics of Road Vehicles*, 4th Edition, SAE International, 1998

[2] Sovran, G., et al. (ed), *Aerodynamic drag mechanisms of Bluff Bodies and Road Vehicles*, Plenum Press, New York, 1978

[3] Hucho, W.H., Sovran, G., *Aerodynamics of Road Vehicles*, Vol. 25: 485-537, 1993

[4] Achenbach, E., *Distribution of Local Pressure and SkinFriction around a Circular Cylinder in Cross-Flow up to 5×10^6*, Journal of Fluid Mechanics, Vol. 34, Pt.4, 1968

[5] Von Karman,Th., *Turbulence and Skin Friction*, Journal of the Aeronautical Sciences, Vol. 1, No 1, pp.1-20, 1934

[6] Anderson, J.D., *Fundamentals of Aerodynamic 3rd Edition*, McGraw-Hill. ISBN 0-07-237335-0, 2001

[7] Jeff Howell, Adrian Gaylard,*" Improving SUV Aerodynamics*", Motor Industry Research association (MIRA) Technical Paper.

[8] P. Gilliron and F. Chometon, *Modeling of Stationary Three-Dimensional Separated Air Flows around an Ahmed Reference Model,* ESAIM: Proc., 1999, Vol. 7, pp. 173-182

[9] Gad-El-Hak M. Modern *developments in flow contro*l. Applied Mechanics Reviews 1996; 9:365–379.

[10] *Gad-El-Hak M, Pollard A, Bonnet J (eds). Flow Control: Fundamentals and Practices.* Springer: Berlin, 1998.

[11] Collis SS, Joslin RD, Seifert A, Theofilis V. *Issues in active flow control: theory, control, simulation*, and experiment. Progress in Aerospace Sciences 2004; 40:237–289.

[12] Bewley T, Liu S. *Optimal and robust control and estimation of linear paths to transition*. Journal of Fluid Mechanics 1998; 365:305–349.

[13] Cathalifaud P, Luchini P. *Optimal control by blowing and suction at the wall of algebraically growing boundary layer disturbances.* In Proceedings of the IUTAM Laminar-turbulent Symposium, V. Sedona, AZ, U.S.A., Saric W, Fasel H (eds). 2002; 307–312

[14] Fournier G, Bourgois S, Pellerin S, Ta Phuoc L, Tensi J, El Jabi R. *Wall suction influence on the flow around a cylinder in laminar wake configuration by large eddy simulation and experimental approaches*. 39e Colloque *d'A´erodynamique Appliquee, Controle des ecoulements*, Mars, Paris, 2004; 22–24..

[15] R. K. Roy, *Design of Experiments Using Taguchi Approach: 16 Steps to Product and Process Improvement*, John Wiley & Sons, New York, NY, USA, 2001.

[16] P. J. Ross, *Taguchi Techniques for Quality Engineering,* Mc-Graw Hill, New York, NY, USA, 1988.

[17] R. S. Rao, C. G. Kumar, R. S. Prakasham, and P. J. Hobbs, "*The Taguchi methodology as a statistical tool for biotechnological applications: a critical appraisal*," Biotechnology Journal, vol. 3, no. 4, pp. 510–523, 2008.

[18] W. Cui, X. Li, S. Zhou, and J. Weng, "*Investigation on process parameters of electrospinning system through orthogonal experimental design,*" Journal of Applied Polymer Science, vol. 103, no. 5, pp. 3105–3112, 2007.

[19] S. Chen, X. Hong, and C. J. Harris, "*Sparse kernel regression modeling using combined locally regularized orthogonal least squares and D-optimality experimental design,*" IEEE Transactions on Automatic Control, vol. 48, no. 6, pp. 1029–1036, 2003.

[20] W. Zhou, X. Zhang, M. Xie, Y. Chen, Y. Li, and G. Duan, "*Infrared-assisted extraction of adenosine from radix isatidis using orthogonal experimental design and LC,*" Chromatographia, vol. 72, no. 7-8, pp. 719–724, 2010.

[21] Ghiasi, H., Pasini, D., and Lessard, L., *Constrained globalized Nelder-Mead method for simultaneous structural and manufacturing optimization of a composite bracket.* J.Compos Mater 42(7):717736, 2008

[22] Lanfrit, M., *Best Practice Guidelines for Handling Automotive External aerodynamics with Fluent*, Version 1.2, http://www.fluentusers.com, 2005